# Superfluidity in Neutron Star Crusts

Nicolas Chamel

Institut d'Astronomie et d'Astrophysique
Université Libre de Bruxelles, Belgium

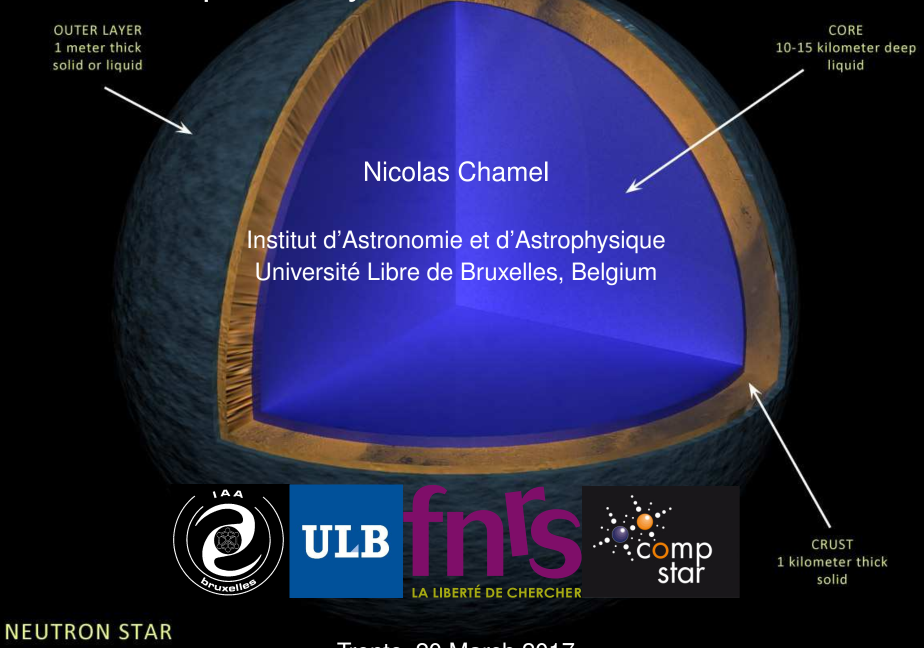


Trento, 20 March 2017

# Outline

1. Observational evidence
2. Superfluid (magneto elasto)hydrodynamics
3. Nuclear energy density functional theory
4. Applications to neutron-star crusts

# Pulsar sudden spin-ups and superfluidity

Pulsars are spinning very rapidly with extremely stable periods:
$\dot{P} \gtrsim 10^{-21}$, as compared to $10^{-18}$ for the best atomic clocks.
*Hinkley et al., Science 341, 1215 (2013).*

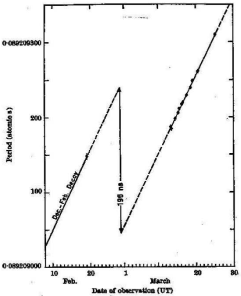


Still, some pulsars have been found to suddenly spin up (in less than a minute).

482 glitches have been detected in 168 pulsars.

`http://www.jb.man.ac.uk/pulsar/glitches.html`

Pulsar glitches provide the strongest evidence of superfluidity in neutron-star crusts.

Neutron-star superfluidity was predicted by Migdal, and first studied by Ginzburg & Kirzhnits before the discovery of pulsars.

# First hints about nuclear superfluidity

The first glitch was detected in Vela in February 1969. At that time, several superconductors were known but the only superfluid was $^4$He.

Cameron & Greenstein considered the onset of **fluid instabilities** assuming "viscous effects to be unimportant" *Nature 222, 862 (May 1969)*

After one year, the spin-down rate relaxed to the value it had before indicating the presence of **superfluidity**.
*Baym, Pethick, Pines, Nature 224, 673 (November 1969)*

In 1972, Packard suggested that glitches are related to the **metastability of the superfluid** (*PRL 28, 1080*).

In 1975, Anderson & Itoh proposed that glitches are triggered by the **unpinning of superfluid vortices in the crust** (*Nature 256, 25*). This model was further developed by Alpar and Pines (Nature 316, 27).

Similar phenomena were observed with superfluid helium.
*J. S. Tsakadze & S. J. Tsakadze, J. Low Temp. Phys. 39, 649 (1980).*

# Other astrophysical manifestations

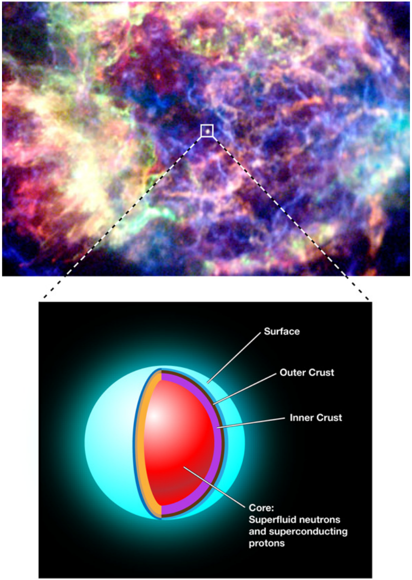


Superfluidity in neutron star crust may leave its imprint on other astrophysical phenomena, such as

- the cooling of young isolated neutron stars,
- the thermal relaxation of transiently accreting neutron stars,
- quasiperiodic oscillations in soft gamma-ray repeaters,
- pulsars free precession.

# Mutual entrainment

In superfluid mixtures such as $^3$He-$^4$He or neutron star cores, the different superfluid constituents can still be **mutually entrained** despite the absence of viscous drag

$$\boldsymbol{j}_\mathbf{X} = \sum_Y n_\mathrm{XY} \boldsymbol{v}_\mathbf{Y} \qquad n_\mathrm{X} = \sum_\mathrm{Y} n_\mathrm{XY}$$

$\boldsymbol{j}_\mathbf{X}$ is the current of the component X
$n_\mathrm{X}$ is the number density of the component X
$\boldsymbol{v}_\mathbf{Y} = \dfrac{\boldsymbol{p}_\mathbf{Y}}{m_\mathrm{Y}}$ is the "superfluid velocity" of the component Y
$n_\mathrm{XY} = n_\mathrm{YX}$ is the entrainment matrix, which depends on the interactions between the constituent particles.

*Andreev & Bashkin, Sov. Phys. JETP 42, 164 (1975).*

In neutron stars, general relativity leads to additional fluid couplings due to frame-dragging effects.
*B. Carter, Ann. Phys. 95, 53 (1975)*
*Sourie et al., MNRAS464, 4641(2017)*

# Entrainment and dissipation in neutron-star cores

Non-dissipative entrainment effects can give rise to friction forces

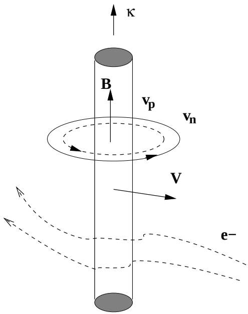


*picture from K. Glampedakis*

Due to entrainment effects, neutron vortices carry a **fractional magnetic quantum flux**

*Sedrakyan and Shakhabasyan, Astrofizika 8 (1972), 557; Astrofizika 16 (1980), 727.*

**The core superfluid is strongly coupled to the crust** due to electrons scattering off the magnetic field of the vortex lines.

*Alpar, Langer, Sauls, ApJ282 (1984) 533*

# Superfluid elastohydrodynamics in neutron-star crusts

In the inner crust of a neutron star, the neutron superfluid is entrained by the lattice of neutron-proton clusters
*Carter, Chamel, Haensel, Nucl.Phys.A748,675(2005)*

$$\boldsymbol{j_n} = n_n^s \boldsymbol{v_n} + (n_n - n_n^s)\boldsymbol{v_p}$$

$n_n^s$ is the **neutron "superfluid" or "conduction" density**
$\boldsymbol{v_n}$ is the neutron "superfluid velocity"
$\boldsymbol{v_p}$ is the velocity of protons (clusters)

The superfluid flow is coupled to the elastic dynamics of the crust

$$M^* \frac{\partial \delta v_{pi}}{\partial t} + (n_n - n_n^s)\nabla_i \delta\mu_n + L\nabla_i \delta n_n - \tilde{K}\nabla_i u_{jj} - 2S\nabla_j(u_{ij} - \delta_{ij}u_{kk}/3) \approx 0$$

$M^* = m(n_p + n_n - n_n^s)$ is the **effective cluster mass**
$u$ is the displacement of clusters about their equilibrium position

*Carter,Chamel,Haensel,Int.J.Mod.Phys.D15,777(2006)*
*Pethick, Chamel, Reddy, Prog.Theor.Phys.Sup.186,9(2010)*

# Variational formulation of superfluid hydrodynamics

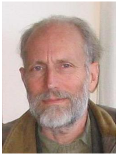

An elegant variational formalism for describing superfluid mixtures in the relativistic context was developed by Brandon Carter using exterior calculus.

*Carter in "Relativistic fluid dynamics" (Springer-Verlag, 1989), pp.1-64*

*Carter, Lect. Notes Phys. 578 (2001), Springer*

This formalism relies on an **action integral** $\mathcal{A} = \int \Lambda\{n_{\rm x}^{\mu}\}\, \mathrm{d}\mathcal{M}^{(4)}$.

The **Lagrangian density** $\Lambda$ depends on the **4-currents** $n_{\rm x}^{\mu} = n_{\rm x} u_{\rm x}^{\mu}$.

It was extended to superfluid (magneto)elastohydrodynamics

*Carter & Samuelsson, Class.Quant. Grav.23, 5367 (2006).*

This formalism was adapted to the Newtonian framework using a fully 4D covariant approach

*Carter&Chamel, Int.J.Mod.Phys.D13,291(2004);D14,717(2005)D14,749(2005)*

*Carter,Chachoua&Chamel, Gen.Rel.Grav.38,83(2006).*

*Carter & Chachoua, Int.J.Mod.Phys.D15, 1329 (2006).*

# Variational formulation of superfluid hydrodynamics

The hydrodynamic equations can be expressed in a very simple form.

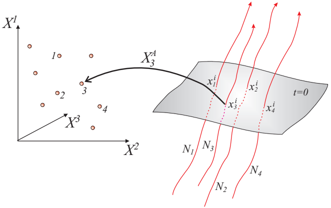


*picture from Andersson&Comer*

Using the action principle and considering variations of the fluid particle trajectories yield

$$n_{\mathrm{x}}^{\mu}\varpi^{\mathrm{x}}_{\mu\nu} + \pi^{\mathrm{x}}_{\nu}\nabla_{\mu} n_{\mathrm{x}}^{\mu} = f^{\mathrm{x}}_{\nu}$$

**4-momentum covector** $$\pi^{\mathrm{x}}_{\mu} = \frac{\partial\Lambda}{\partial n_{\mathrm{x}}^{\mu}}$$

**vorticity 2-form** $$\varpi^{\mathrm{x}}_{\mu\nu} = 2\nabla_{[\mu}\pi^{\mathrm{x}}_{\nu]} = \nabla_{\mu}\pi^{\mathrm{x}}_{\nu} - \nabla_{\nu}\pi^{\mathrm{x}}_{\mu}$$

**4-force density covector** $$f^{\mathrm{x}}_{\nu}$$

With this approach, conservation laws can be easily derived.

# Example: generalized Kutta-Joukowski theorem

**Lift force** per unit length acting on a **straight vortex line** immersed in an asymptotically uniform medium with currents $\overline{n_{\rm x}}^{\nu}$:

$$\mathcal{F}_\nu \stackrel{\star}{=} \varepsilon_{\sigma\nu} \sum_{\rm x} \mathcal{C}^{\rm x} \overline{n_{\rm x}}^{\sigma} \qquad \mathcal{C}^{\rm x} = \oint \pi^{\rm x}_{\nu}\, dx^{\nu}$$

*Carter&Chamel, Int.J.Mod.Phys.D14,717(2005)*

Application to Tisza-Landau's two fluid model:

$$\boldsymbol{\mathcal{F}} = \underbrace{\rho\boldsymbol{\kappa}\times(\boldsymbol{v_L}-\boldsymbol{v_S})}_{\rm Magnus} + \underbrace{\rho_N\boldsymbol{\kappa}\times(\boldsymbol{v_S}-\boldsymbol{v_N})}_{\rm Iordanskii} + \underbrace{C(T)\boldsymbol{\kappa}\times(\boldsymbol{v_L}-\boldsymbol{v_N})}_{\rm Kopnin-Kravtsov}$$

$\boldsymbol{v_S}$ is the "superfluid velocity"
$\boldsymbol{v_N}$ is the velocity of the "normal" component
$\boldsymbol{v_L}$ is the vortex line velocity

The Kopnin parameter is $C(T) = \dfrac{s\mathcal{C}}{\kappa}$, where $s$ is the entropy density and $\mathcal{C}$ is the momentum circulation of the "normal" component.

# Nuclear energy density functional theory in a nut shell

The energy $E$ of a nuclear system ($q = n, p$ for neutrons, protons) is expressed as a (universal) functional of

- $n_q(\boldsymbol{r}, \sigma; \boldsymbol{r'}, \sigma') =< \Psi | c_q(\boldsymbol{r'}\sigma')^\dagger c_q(\boldsymbol{r}\sigma) | \Psi >$
- $\widetilde{n}_q(\boldsymbol{r}, \sigma; \boldsymbol{r'}, \sigma') = -\sigma' < \Psi | c_q(\boldsymbol{r'} - \sigma') c_q(\boldsymbol{r}\sigma) | \Psi >$,

where $c_q(\boldsymbol{r}\sigma)^\dagger$ and $c_q(\boldsymbol{r}\sigma)$ are the creation and destruction operators for nucleon $q$ at position $\boldsymbol{r}$ with spin $\sigma = \pm 1$.

In turn, these matrices are expressed in terms of **independent quasiparticle** wavefunctions $\varphi_{1k}^{(q)}(\boldsymbol{r})$ and $\varphi_{2k}^{(q)}(\boldsymbol{r})$ as

$$n_q(\boldsymbol{r}, \sigma; \boldsymbol{r'}, \sigma') = \sum_{k(q)} \varphi_{2k}^{(q)}(\boldsymbol{r}, \sigma) \varphi_{2k}^{(q)}(\boldsymbol{r'}, \sigma')^*$$

$$\widetilde{n}_q(\boldsymbol{r}, \sigma; \boldsymbol{r'}, \sigma') = -\sum_{k(q)} \varphi_{2k}^{(q)}(\boldsymbol{r}, \sigma) \varphi_{1k}^{(q)}(\boldsymbol{r'}, \sigma')^* = -\sum_{k} \varphi_{1k}^{(q)}(\boldsymbol{r}, \sigma) \varphi_{2k}^{(q)}(\boldsymbol{r'}, \sigma')^* .$$

The ***exact* ground-state energy** is obtained by minimizing the functional $E[n_q(\boldsymbol{r}, \sigma; \boldsymbol{r'}, \sigma'), \widetilde{n}_q(\boldsymbol{r}, \sigma; \boldsymbol{r'}, \sigma')]$ under the constraint of fixed nucleon numbers (and completeness relations on $\varphi_{1k}^{(q)}(\boldsymbol{r})$ and $\varphi_{2k}^{(q)}(\boldsymbol{r})$).

# Skyrme effective nucleon-nucleon interactions

We have constructed phenomenological functionals from **generalized Skyrme effective nucleon-nucleon interactions** in the "mean-field" approximation

$$v_{ij} = t_0(1+x_0P_\sigma)\delta(\boldsymbol{r}_{ij}) + \frac{1}{2}t_1(1+x_1P_\sigma)\frac{1}{\hbar^2}\left[p_{ij}^2\,\delta(\boldsymbol{r}_{ij}) + \delta(\boldsymbol{r}_{ij})\,p_{ij}^2\right]$$
$$+t_2(1+x_2P_\sigma)\frac{1}{\hbar^2}\boldsymbol{p}_{ij}.\delta(\boldsymbol{r}_{ij})\,\boldsymbol{p}_{ij} + \frac{1}{6}t_3(1+x_3P_\sigma)n(\boldsymbol{r})^\alpha\,\delta(\boldsymbol{r}_{ij})$$
$$+\frac{1}{2}\,t_4(1+x_4P_\sigma)\frac{1}{\hbar^2}\left\{p_{ij}^2\,n(\boldsymbol{r})^\beta\,\delta(\boldsymbol{r}_{ij}) + \delta(\boldsymbol{r}_{ij})\,n(\boldsymbol{r})^\beta\,p_{ij}^2\right\}$$
$$+t_5(1+x_5P_\sigma)\frac{1}{\hbar^2}\boldsymbol{p}_{ij}\cdot n(\boldsymbol{r})^\gamma\,\delta(\boldsymbol{r}_{ij})\,\boldsymbol{p}_{ij}$$
$$+\frac{\mathrm{i}}{\hbar^2}W_0(\boldsymbol{\sigma_i}+\boldsymbol{\sigma_j})\cdot\boldsymbol{p}_{ij}\times\delta(\boldsymbol{r}_{ij})\,\boldsymbol{p}_{ij} + \frac{\mathrm{i}}{\hbar^2}W_1(\boldsymbol{\sigma}_i+\boldsymbol{\sigma}_j)\cdot\boldsymbol{p}_{ij}\times(n_{qi}+n_{qj})^\nu\,\delta(\boldsymbol{r}_{ij})\,\boldsymbol{p}_{ij}$$

$$\textbf{pairing}\quad v_{ij}^\pi = \frac{1}{2}(1+P_\sigma)v^\pi[n_n(\boldsymbol{r}), n_p(\boldsymbol{r}), \nabla n_n(\boldsymbol{r}), \nabla n_p(\boldsymbol{r})]\delta(\boldsymbol{r}_{ij})$$

$\boldsymbol{r}_{ij} = \boldsymbol{r}_i - \boldsymbol{r}_j$, $\boldsymbol{r} = (\boldsymbol{r}_i + \boldsymbol{r}_j)/2$, $\boldsymbol{p}_{ij} = -\mathrm{i}\hbar(\boldsymbol{\nabla}_i - \boldsymbol{\nabla}_j)/2$ is the relative momentum, and $P_\sigma$ is the two-body spin-exchange operator.

The parameters $t_i$, $x_i$, $\alpha$, $\beta$, $\gamma$, $\nu$, $W_i$ must be fitted to experimental and/or microscopic nuclear data.

# Hartree-Fock-Bogoliubov equations

Minimizing $E\left[\varphi_{1k}^{(q)}(\boldsymbol{r}), \varphi_{2k}^{(q)}(\boldsymbol{r})\right]$ under the constraint of fixed nucleon numbers leads to the **Bogoliubov-De Gennes** equations:

$$\sum_{\sigma'} \begin{pmatrix} h_q(\boldsymbol{r})_{\sigma\sigma'} & \Delta_q(\boldsymbol{r})\delta_{\sigma\sigma'} \\ \Delta_q(\boldsymbol{r})\delta_{\sigma\sigma'} & -h_q(\boldsymbol{r})_{\sigma\sigma'} \end{pmatrix} \begin{pmatrix} \varphi_{1k}^{(q)}(\boldsymbol{r}, \sigma') \\ \varphi_{2k}^{(q)}(\boldsymbol{r}, \sigma') \end{pmatrix} = E_k \begin{pmatrix} \varphi_{1k}^{(q)}(\boldsymbol{r}, \sigma) \\ \varphi_{2k}^{(q)}(\boldsymbol{r}, \sigma) \end{pmatrix}$$

$$h_q(\boldsymbol{r})_{\sigma'\sigma} \equiv -\boldsymbol{\nabla} \cdot \frac{\delta E}{\delta \tau_q(\boldsymbol{r})} \boldsymbol{\nabla} \delta_{\sigma\sigma'} + \frac{\delta E}{\delta n_q(\boldsymbol{r})} \delta_{\sigma\sigma'} - \mathrm{i} \frac{\delta E}{\delta \boldsymbol{J}_q(\boldsymbol{r})} \cdot \boldsymbol{\nabla} \times \boldsymbol{\sigma}_{\sigma'\sigma} - \mu_q \delta_{\sigma\sigma'},$$

$\mu_q$ are the nucleon chemical potentials,

$\Delta_q(\boldsymbol{r}) \equiv \dfrac{\delta E}{\delta \tilde{n}_q(\boldsymbol{r})}$ is called the pair potential or the pairing field.

*Duguet, Lecture Notes in Physics 879 (Springer-Verlag, 2014), p. 293*

*Dobaczewski & Nazarewicz, in "50 years of Nuclear BCS" (World Scientific Publishing, 2013), pp.40-60*

# Brussels-Montreal Skyrme functionals (BSk)

**Experimental data**:

- all atomic masses with $Z, N \geq 8$ from the Atomic Mass Evaluation (root-mean square deviation: 0.5-0.6 MeV)
- nuclear charge radii
- symmetry energy $29 \leq J \leq 32$ MeV
- incompressibility $K_v = 240 \pm 10$ MeV (ISGMR)
  *Colò et al., Phys.Rev.C70, 024307 (2004).*

**N-body calculations using realistic forces**:

- equation of state of pure neutron matter
- $^1S_0$ pairing gaps in nuclear matter
- effective masses in nuclear matter
- stability against spin and spin-isospin fluctuations

Nonlocal and relativistic functionals have been developed:
*Goriely et al., Eur. Phys. J. A 52, 202 (2016).*
*Pena Arteaga, Goriely, Chamel, Eur. Phys. J. A 52, 320 (2016)*

# Pairing functionals from nuclear-matter calculations

Pairing is described by functionals of the form

$$E_{\rm pair} = \int d^3r\, \mathcal{E}_{\rm pair}(\boldsymbol{r})\,, \quad \mathcal{E}_{\rm pair} = \frac{1}{4}\sum_{q=n,p} v^{\pi q}[n_n, n_p]\tilde{n}_q^2$$

with a cutoff prescription to avoid divergences.

$v^{\pi q}[n_n, n_p]$ is determined so as to reproduce exactly $^1S_0$ pairing gaps $\Delta_q(n_n, n_p)$ in nuclear matter (cutoff $\varepsilon_\Lambda$ above the Fermi level) :

$$v^{\pi q} = -8\pi^2 \left(\frac{\hbar^2}{2M_q^*}\right)^{3/2} \left(\int_0^{\mu_q+\varepsilon_\Lambda} \frac{\sqrt{\varepsilon}\mathrm{d}\varepsilon}{\sqrt{(\varepsilon-\mu_q)^2+\Delta_q^2}}\right)^{-1}$$

$$\frac{\hbar^2}{2M_q^*} \equiv \frac{\delta E}{\delta \tau_q}$$

*Chamel, Goriely, Pearson, Nucl. Phys.A812,72 (2008).*

# Analytical expression of the pairing strength

In the "weak-coupling approximation" $\Delta_q \ll \mu_q$ and $\Delta_q \ll \varepsilon_\Lambda$,

$$v^{\pi q} = -\frac{8\pi^2}{\sqrt{\mu_q}} \left(\frac{\hbar^2}{2M_q^*}\right)^{3/2} \left[2\log\left(\frac{2\mu_q}{\Delta_q}\right) + \Lambda\left(\frac{\varepsilon_\Lambda}{\mu_q}\right)\right]^{-1}$$

$$\Lambda(x) = \log(16x) + 2\sqrt{1+x} - 2\log\left(1+\sqrt{1+x}\right) - 4$$

$$\mu_q = \frac{\hbar^2}{2M_q^*}(3\pi^2 n_q)^{2/3}$$

*Chamel, Phys. Rev. C 82, 014313 (2010)*

- **realistic pairing gaps** in homogeneous nuclear matter
- **no free parameters** apart from the cutoff
- **automatic renormalization** of the pairing strength with $\varepsilon_\Lambda$

# Pairing cutoff and experimental phase shifts

In the limit of vanishing density, the pairing strength

$$v^{\pi q}[n_n, n_p \to 0] = -\frac{4\pi^2}{\sqrt{\varepsilon_\Lambda}}\left(\frac{\hbar^2}{2M_q}\right)^{3/2}$$

should coincide with the bare force in the ${}^1S_0$ channel.

A fit to the **experimental ${}^1\mathbf{S}_0$ NN phase shifts** yields $\varepsilon_\Lambda \sim 7 - 8$ MeV.
*Esbensen et al., Phys. Rev. C 56, 3054 (1997).*

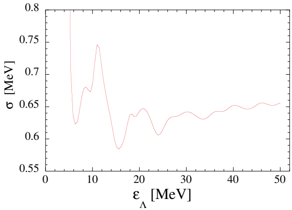


The fit to nuclear masses leads to a non monotonic dependence of the rms error on the cutoff.
*Chamel et al., in "50 Years of Nuclear BCS" (World Scientific Publishing Company, 2013), pp.284-296*

For the functionals BSk16-BS29, optimum mass fits were obtained with $\varepsilon_\Lambda \sim 16$ MeV, while we found $\varepsilon_\Lambda \sim 6.5$ MeV for BSk30-32.

# Other contributions to pairing in finite nuclei

Pairing in finite nuclei is not expected to be the same as in infinite nuclear matter because of

- **Coulomb and charge symmetry breaking effects**,
- **polarization effects in odd nuclei** (we use the equal filling approximation),
- **coupling to surface vibrations**.

In an attempt to account for these effects, we include an additional phenomenological term in the pairing functional (only for BSk30-32)

$$v^{\pi\, q} \rightarrow v^{\pi\, q} + \kappa_q |\nabla n|^2$$

and we introduce renormalization factors $f_q^{\pm}$

$$v^{\pi\, q} \longrightarrow f_q^{\pm} v^{\pi\, q} \ ,$$

Typically $f_q^{\pm} \simeq 1 - 1.2$ and $f_q^{-} > f_q^{+}$, and $\kappa_q < 0$.

# $^1S_0$ pairing gaps in nuclear matter

For consistency, we considered the gaps obtained from extended BHF calculations since effective masses as well as equations of state have been also calculated with this approach.

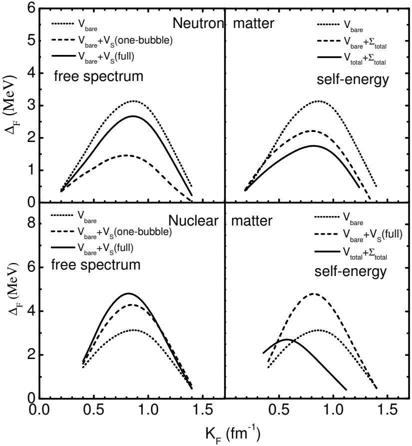


For comparison, we fitted functionals to different approximations for the gaps:

- **BCS**: BSk16
- **polarization+free spectrum**: BSk17-BSk29
- **polarization+self-energy**: BSk30-32.

*Cao et al., Phys.Rev.C74,064301(2006)*

# Nucleon effective masses

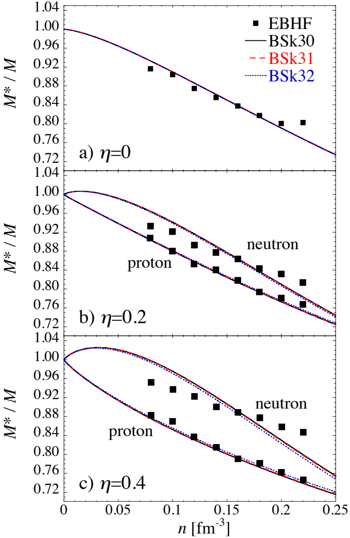


Effective masses obtained with our functionals are consistent with giant resonances in finite nuclei and many-body calculations in infinite nuclear matter.

This was achieved using **generalized Skyrme interactions** with density dependent $t_1$ and $t_2$ terms, initially introduced to remove spurious instabilities.
*Chamel, Goriely, Pearson, Phys.Rev.C80,065804(2009)*

EBHF calculations from *Cao et al.,Phys.Rev.C73,014313(2006)*.

# DFT in neutron-star crusts

The structure of the crust is not a priori known, and has to be determined treating consistently both clusters and free neutrons.

The full implementation of the DFT is computationally very expensive because of the large number of nucleons in the Wigner-Seitz cell ($\sim 10^2 - 10^3$).

We thus proceed in two steps:

1. the equilibrium structure of the crust is determined using the **Extended Thomas-Fermi+Strutinsky Integral** approach:
   - nucleon densities $n_q(\boldsymbol{r})$ are taken as basic variables,
   - clusters are supposed to be spherical (no pastas) and $n_q(\boldsymbol{r})$ are parametrized,
   - proton shell effects are added perturbatively (neutron shell effects are much smaller and therefore neglected).

   *Pearson,Chamel,Pastore,Goriely,Phys.Rev.C91, 018801 (2015).*
2. the neutron superfluid properties are computed from **band-structure calculations**.

# Structure of neutron star crusts

With increasing density, the clusters keep essentially the same size but become more and more dilute.

The crust-core transition predicted by the ETFSI method agrees very well with the instability analysis of homogeneous nuclear matter.

| | $\bar{n}_{\rm cc}$ (fm$^{-3}$) | $P_{\rm cc}$ (MeV fm$^{-3}$) |
|---|---|---|
| BSk21 | 0.0809 | 0.268 |
| BSk20 | 0.0854 | 0.365 |
| BSk19 | 0.0885 | 0.428 |

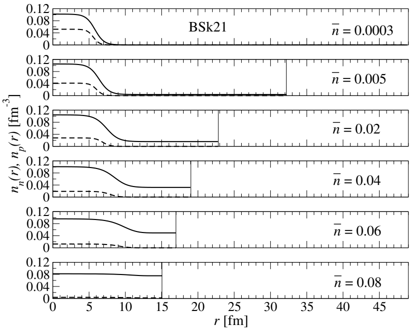


*Pearson,Chamel,Goriely,Ducoin,Phys.Rev.C85,065803(2012).*

The crust-core transition is of very weak first order.

# Band theory

**Floquet-Bloch theorem**

> *I found to my delight that the wave differed from the plane wave of free electrons only by a periodic modulation.*

*Bloch, Physics Today 29 (1976), 23-27.*

The single-particle wave functions can be expressed as

$$\varphi_{\alpha\boldsymbol{k}}(\boldsymbol{r}) = e^{\mathrm{i}\,\boldsymbol{k}\cdot\boldsymbol{r}} u_{\alpha\boldsymbol{k}}(\boldsymbol{r})$$

where $u_{\alpha\boldsymbol{k}}(\boldsymbol{r}+\boldsymbol{\ell}) = u_{\alpha\boldsymbol{k}}(\boldsymbol{r})$ and $\boldsymbol{\ell}$ are lattice vectors.

- $\alpha$ (band index) accounts for the rotational symmetry around each lattice site,
- $\boldsymbol{k}$ (wave vector) accounts for the translational symmetry of the crystal.

*Chamel, Goriely, Pearson, in "50 years of Nuclear BCS" (World Scientific Publishing, 2013), pp.284-296.*

# Band theory

By symmetry, the crystal can be partitioned into identical primitive cells. The HFB equations need to be solved only inside one cell.

- The shape of the cell depends on the crystal symmetry

Example : body centered cubic lattice

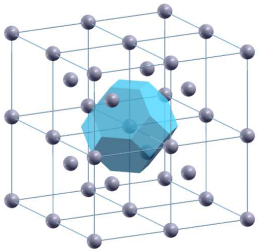

- The boundary conditions are fixed by the Floquet-Bloch theorem

$$\varphi_{\alpha \boldsymbol{k}}(\boldsymbol{r}+\boldsymbol{\ell}) = e^{\mathrm{i}\,\boldsymbol{k}\cdot\boldsymbol{\ell}}\varphi_{\alpha \boldsymbol{k}}(\boldsymbol{r})$$

- $\boldsymbol{k}$ can be restricted to the first Brillouin zone (primitive cell of the reciprocal lattice) since for any reciprocal lattice vector $\boldsymbol{K}$

$$\varphi_{\alpha \boldsymbol{k}+\boldsymbol{K}}(\boldsymbol{r}) = \varphi_{\alpha \boldsymbol{k}}(\boldsymbol{r})$$

# Multiband BCS theory

In the deep layers of the crusts, the spatial fluctuations of $\Delta(\boldsymbol{r})$ are small compared to those of $\varphi_{\alpha\boldsymbol{k}}(\boldsymbol{r})$ so that

$$\int \mathrm{d}^3\boldsymbol{r}\, \varphi^*_{\alpha\boldsymbol{k}}(\boldsymbol{r})\Delta(\boldsymbol{r})\varphi_{\beta\boldsymbol{k}}(\boldsymbol{r}) \approx \delta_{\alpha\beta} \int \mathrm{d}^3\boldsymbol{r}\, |\varphi_{\alpha\boldsymbol{k}}(\boldsymbol{r})|^2\Delta(\boldsymbol{r})\,.$$

In this decoupling approximation, the Hartree-Fock-Bogoliubov equations reduce to the **multi-band BCS equations**:

$$\Delta_{\alpha\boldsymbol{k}} = -\frac{1}{2}\sum_{\beta}\int \frac{\mathrm{d}^3\boldsymbol{k'}}{(2\pi)^3}\,\bar{v}^{\rm pair}_{\alpha\boldsymbol{k}\alpha-\boldsymbol{k}\beta\boldsymbol{k'}\beta-\boldsymbol{k'}}\,\frac{\Delta_{\beta\boldsymbol{k'}}}{E_{\beta\boldsymbol{k'}}}\tanh\frac{E_{\beta\boldsymbol{k'}}}{2k_{\rm B}T}$$

$$\bar{v}^{\rm pair}_{\alpha\boldsymbol{k}\alpha-\boldsymbol{k}\beta\boldsymbol{k'}\beta-\boldsymbol{k'}} = \int \mathrm{d}^3r\, v^{\pi}[\rho_n(\boldsymbol{r}),\rho_p(\boldsymbol{r})]\,|\varphi_{\alpha\boldsymbol{k}}(\boldsymbol{r})|^2|\varphi_{\beta\boldsymbol{k'}}(\boldsymbol{r})|^2$$

$$E_{\alpha\boldsymbol{k}} = \sqrt{(\varepsilon_{\alpha\boldsymbol{k}}-\mu)^2+\Delta^2_{\alpha\boldsymbol{k}}}$$

$\varepsilon_{\alpha\boldsymbol{k}}$, $\mu$ and $\varphi_{\alpha\boldsymbol{k}}(\boldsymbol{r})$ are obtained from band structure calculations using the ETFSI mean fields

*Chamel et al., Phys.Rev.C81,045804 (2010).*

# Neutron superfluidity in neutron-star crusts

The superfluid permeates the clusters due to proximity effects.

Neutron pairing field for $\bar{n} = 0.06$ fm$^{-3}$ at $T = 0$:

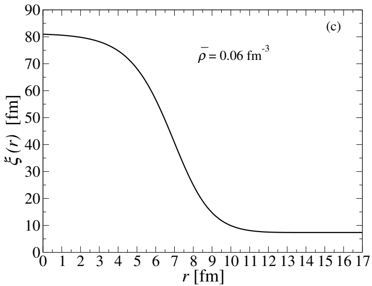


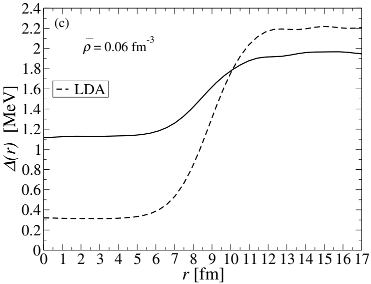


- $\Delta_{\alpha\boldsymbol{k}}(T)/\Delta_{\alpha\boldsymbol{k}}(0)$ is a universal function of $T$
- The critical temperature is approximately given by the usual BCS relation $T_\mathrm{c} \simeq 0.567\Delta_\mathrm{F}$
- the nuclear clusters lower the gap by $10 - 20\%$

# Neutron superfluidity in neutron-star crusts

The superfluid permeates the clusters due to proximity effects.

Neutron pairing field for $\bar{n} = 0.06$ fm$^{-3}$ at $T > 0$:

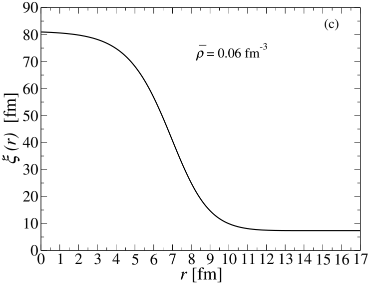


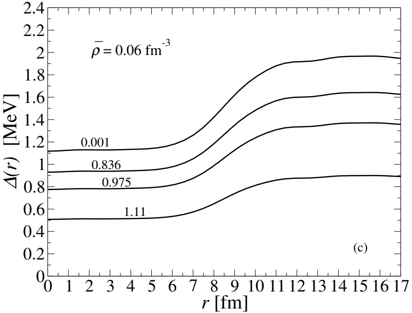


- $\Delta_{\alpha\boldsymbol{k}}(T)/\Delta_{\alpha\boldsymbol{k}}(0)$ is a universal function of $T$
- The critical temperature is approximately given by the usual BCS relation $T_{\rm c} \simeq 0.567\Delta_{\rm F}$
- the nuclear clusters lower the gap by $10-20\%$

# How “free” are neutrons in the crust?

**Hydrodynamic approach:**

- superfluid neutrons flowing through a lattice of clusters
- a fraction $\delta$ of neutrons in clusters are superfluid

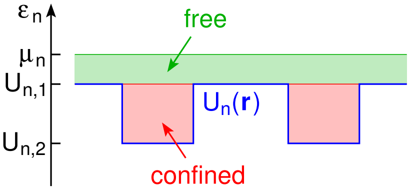


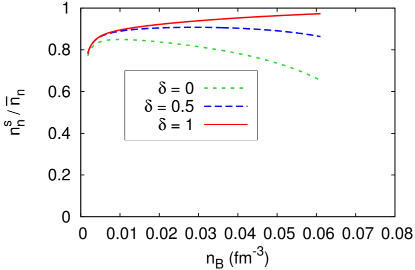


*Martin&Urban,Phys.Rev.C94, 065801 (2016)*
*Magierski&Bulgac,Act.Phys.Pol.B35,1203 (2004)*
*Magierski, Int. J. Mod. Phys. E13, 371 (2004)*
*Sedrakian, Astrophys. Spa. Sci.236, 267 (1996)*

Limitation: coherence length $\xi$ must be much smaller than cluster size

# Neutron "conduction" from the band theory

In the BCS regime, the "superfluid" neutron density is given by

$$n_n^s = \frac{m_n}{24\pi^3\hbar^2}\sum_\alpha \int |\nabla_{\boldsymbol{k}}\varepsilon_{\alpha\boldsymbol{k}}|^2 \frac{\Delta_{\alpha\boldsymbol{k}}}{E_{\alpha\boldsymbol{k}}}\mathrm{d}^3k \qquad E_{\alpha\boldsymbol{k}} = \sqrt{(\varepsilon_{\alpha\boldsymbol{k}}-\mu)^2+\Delta_{\alpha\boldsymbol{k}}^2}$$

In the weak coupling limit $\Delta_{\alpha\boldsymbol{k}} \ll \mu$,

$$n_n^s \approx \frac{m_n}{24\pi^3\hbar^2}\sum_\alpha \int_{\mathrm{F}} |\nabla_{\boldsymbol{k}}\varepsilon_{\alpha\boldsymbol{k}}|\mathrm{d}\mathcal{S}^{(\alpha)}$$

*Carter,Chamel,Haensel.Nucl.Phys.A748,675 (2005)*
*Carter,Chamel,Haensel.Nucl.Phys.A759,441(2005)*

The neutron conduction depends on the shape of the Fermi surface:

- spherical Fermi surface $n_n^s = n_n^f$
  all unbound neutrons are free (metal)
- no Fermi surface (band gap) $n_n^s = 0$
  all unbound neutrons are entrained (insulator).

# Neutron band structure: shallow region

Neutron band structure (s.p. energy in MeV vs $\boldsymbol{k}$) with (left) and without (right) a bcc lattice at $\bar{n} = 0.0003$ fm$^{-3}$ ($Z = 50, A = 200$):

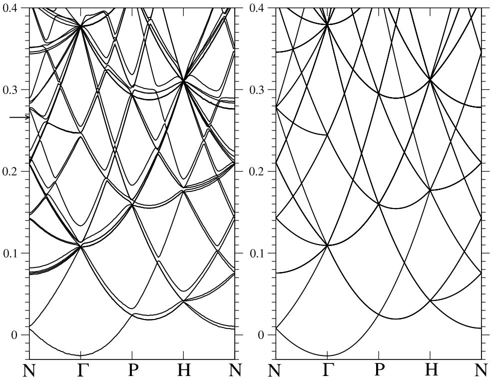


*Chamel,Phys.Rev.C85,035801(2012).*

The band structure is similar to that of free neutrons: entrainment is therefore expected to be weak.

# Neutron Fermi surface

Example at $\bar{n} = 0.0003$ fm$^{-3}$ (reduced zone scheme)

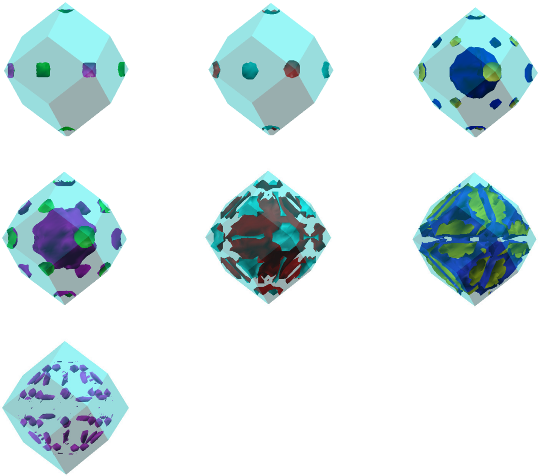

# Neutron band structure: intermediate region

Neutron band structure (s.p. energy in MeV vs $\boldsymbol{k}$) with (left) and without (right) a bcc lattice at $\bar{n} = 0.03$ fm$^{-3}$ ($Z = 40, A = 1590$):

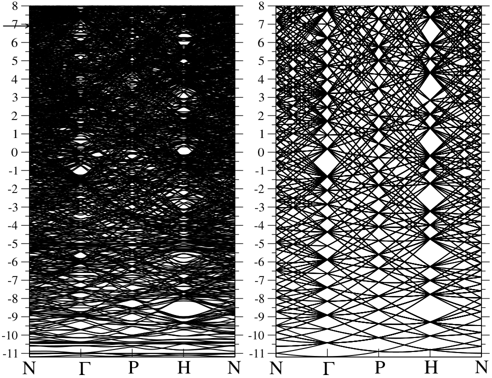


*Chamel,Phys.Rev.C85,035801(2012).*

The band structure is very different from that of free neutrons: entrainment is therefore expected to be strong.

# Neutron band structure: deep region

Neutron band structure (s.p. energy in MeV vs $\boldsymbol{k}$) with (left) and without (right) a bcc lattice at $\bar{n} = 0.08$ fm$^{-3}$ ($Z = 20, A = 665$):

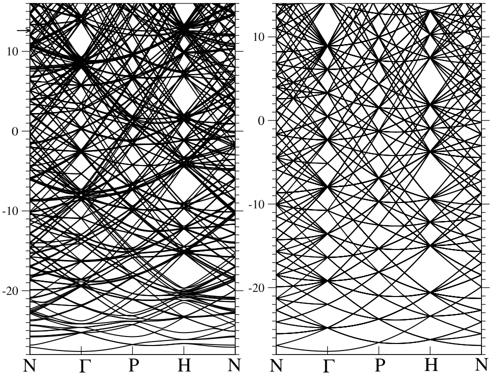


*Chamel,Phys.Rev.C85,035801(2012).*

The band structure is similar that of free neutrons: entrainment is therefore expected to be weak.

# How “free” are neutrons in neutron-star crusts?

Systematic band structure calculations from the neutron-drip transition to the crust-core boundary.

$n_n$ is the total neutron density
$n_n^f$ is the unbound neutron density
$n_n^s$ is the “conduction” neutron density

| $\bar{n}$ (fm$^{-3}$) | $n_n^f/n_n$ (%) | $n_n^s/n_n^f$ (%) |
|---|---|---|
| 0.0003 | 20.0 | 82.6 |
| 0.001 | 68.6 | 27.3 |
| 0.005 | 86.4 | 17.5 |
| 0.01 | 88.9 | 15.5 |
| 0.02 | 90.3 | 7.37 |
| 0.03 | 91.4 | 7.33 |
| 0.04 | 88.8 | 10.6 |
| 0.05 | 91.4 | 30.0 |
| 0.06 | 91.5 | 45.9 |
| 0.08 | 104 | 64.8 |

*Chamel,Phys.Rev.C85,035801(2012)*

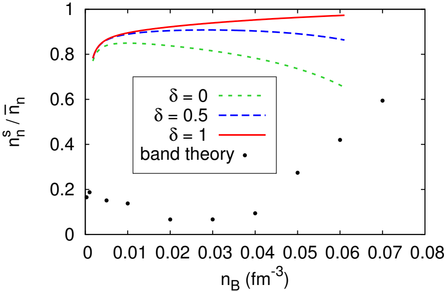


*Martin&Urban,Phys.Rev.C94, 065801 (2016)*

Entrainment effects predicted by the band theory are much stronger than obtained by the hydrodynamic approach.

# Role of quantum zero point motion and pairing

*Preliminary* band-structure calculations including

- quantum-zero point motion of ions with bare ion mass $M$
- constant BCS pairing ($\Delta_{\alpha\boldsymbol{k}} = \Delta$ ranging from $\sim 0$ to $\sim 3$ MeV)

$m_n^\star/m_n = n_n^f/n_n^s$

static lattice

| $\bar{n}$ (fm$^{-3}$) | $m_n^\star/m_n$ |
|---|---|
| 0.02 | 13.7 |
| 0.03 | 12.7 |
| 0.04 | 9 |
| 0.05 | 2.8 |
| 0.06 | 1.8 |
| 0.07 | 1.2 |

with Debye-Waller (DW)

| $\bar{n}$ (fm$^{-3}$) | $m_n^\star/m_n$ |
|---|---|
| 0.02 | 13.7 |
| 0.03 | 12.3 |
| 0.04 | 8.1 |
| 0.05 | 2.2 |
| 0.06 | 1.5 |
| 0.07 | 1.1 |

with DW+BCS pairing

| $\bar{n}$ (fm$^{-3}$) | $m_n^\star/m_n$ |
|---|---|
| 0.02 | 15.8 |
| 0.03 | 13.5 |
| 0.04 | 8.2 |
| 0.05 | 2.3 |
| 0.06 | 1.5 |
| 0.07 | 1.1 |

In reality, ion motion itself is suppressed by entrainment
$\langle u^2 \rangle \propto 1/\sqrt{M^*}$ since $M^* > M$.

The **superfluid still remains strongly coupled to the crust.**

# Entrainment and collective excitations

Entrainment impacts low-energy collective excitations:

- clusters are effectively heavier $M^* > M$,
- lattice and superfluid longitudinal excitations are mixed.

*Chamel,Page,Reddy,Phys.Rev.C87,035803(2013)*
*Chamel,Page,Reddy,J.Phys. Conf.Ser.665, 012065 (2016).*

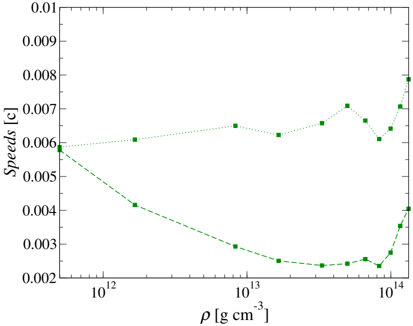


Transverse lattice phonon speeds with (dashed line) and without (dotted line) entrainment.

# Entrainment and collective excitations

Entrainment impacts low-energy collective excitations:

- clusters are effectively heavier $M^* > M$,
- lattice and superfluid longitudinal excitations are mixed.

*Chamel,Page,Reddy,Phys.Rev.C87,035803(2013)*
*Chamel,Page,Reddy,J.Phys. Conf.Ser.665, 012065 (2016).*

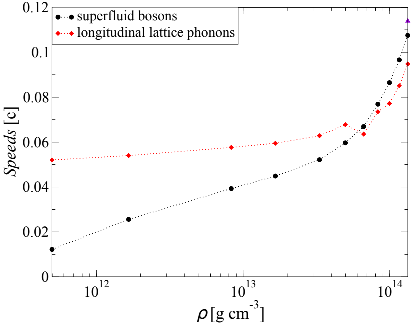


No entrainment, no mixing

# Entrainment and collective excitations

Entrainment impacts low-energy collective excitations:

- clusters are effectively heavier $M^* > M$,
- lattice and superfluid longitudinal excitations are mixed.

*Chamel,Page,Reddy,Phys.Rev.C87,035803(2013)*
*Chamel,Page,Reddy,J.Phys. Conf.Ser.665, 012065 (2016).*

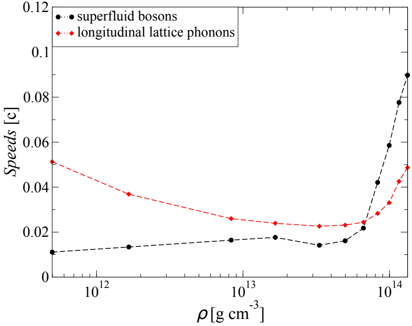


Entrainment, no mixing

# Entrainment and collective excitations

Entrainment impacts low-energy collective excitations:

- clusters are effectively heavier $M^* > M$,
- lattice and superfluid longitudinal excitations are mixed.

*Chamel,Page,Reddy,Phys.Rev.C87,035803(2013)*
*Chamel,Page,Reddy,J.Phys. Conf.Ser.665, 012065 (2016).*

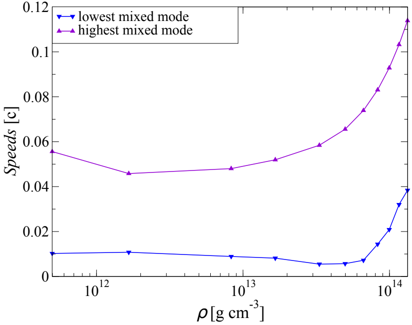


Entrainment and mixing

# Conclusions

- **Giant pulsar glitches** provide the strongest evidence of superfluidity in neutron-star crusts.
- The (non)relativistic superfluid (magneto elasto)hydrodynamic equations can be derived from an **action principle**.
- We have calculated the structure of the crust from the **nuclear energy density functional theory** using the ETFSI approach.
- We have determined the superfluid properties (pairing gaps, “superfluid” density) by employing the **band theory** of solids.

The neutron superfluid is found to be strongly coupled to the crust; this may have implications for various astrophysical phenomena (glitches, QPOs, cooling).